AIAA JOURNAL
Vol. 30, No. 4, April 1992

Flow Near the Trailing Edge of an Airfoil

Lucien Z. Dumitrescu*
Institute of Aeronautics, 79622 Bucharest, Romania

Some theorems are established for the slope and curvature radius of an airfoil contour obtained by conformal mapping, the velocity gradient along it, and the curvature of streamlines. Following a discussion on some general features of the conformal mapping for a wide range of airfoil shapes, the flow behavior near the trailing edge is carefully examined. It is shown that, in potential flow, the emerging streamline there has infinite curvature, except at a singular angle of attack. One infers that the interplay between the external flow and the boundary layer will produce, at each flow regime, an equivalent airfoil contour (with the displacement thickness added), having such a shape at the trailing edge that its singular angle of attack, rendering the streamline curvature finite, would coincide with the actual incidence. This might require a certain amount of separation; therefore, by suitably shaping the trailing edge of the real airfoil, e.g., with a small moving tab, one may alter the contour to avoid detachment, and thereby reduce cruise drag by a few percent.

I. Introduction

NOWADAYS, solutions to airfoil flow problems are commonly found with numerical methods, which carry out manipulations of local variables in a multitude of points throughout the flowfield. It is a pity that this recourse to brute computer force has sent into oblivion the more traditional approach, which seeks, with the help of conformal mapping and complex potentials, global solutions, valid in the whole domain and correctly representing the asymptotic conditions. Judicious use of modern computing tools multiplies the power of these methods and, as we shall try to illustrate hereafter, permits us to study the fine details of the flow, while also gaining insight into some important qualitative aspects, which are obscured by the "pointillist" way of painting the reality. Of particular interest is the behavior of the flow near the trailing edge since it determines the circulation (and influences also the drag); this is even more important for unsteady flows. Our endeavor will be, therefore, to show how the appliction of certain theorems on conformal mapping and potential flow throws new lights on these classical problems and suggests interesting developments.

II. Two Theorems on Conformal Mapping

We shall start with the following problem: let Γ be a contour, in the complex plane $\zeta=\xi+i\eta$, and C its image, in the plane $z=x+iy$, through a conformal mapping function $z=f(\zeta)$ (Figs. 1). Let also $\bar{\tau}$, $\bar{t}$ and $\bar{\rho}$, $\bar{r}$ be, respectively, the local tangent angles and radii of curvature at two corresponding points A, A' along Γ and C. Is it possible to write down a relationship between $\bar{\tau}$ and $\bar{t}$, and one between $\bar{\rho}$ and $\bar{r}$, if $f(\zeta)$ is known? The answer is yes, and is obtained as follows:

First, we write down the local differentials along the curves

$$d\zeta = d\sigma \exp(i\bar{\tau}), \qquad dz = ds \exp(i\bar{t}) \tag{1}$$

or

$$f' = \frac{dz}{d\zeta} = \frac{ds}{d\sigma}\exp\left[i(\bar{t}-\bar{\tau})\right] \tag{2}$$

where σ and s are the curvilinear abscissas along Γ and C.

A *first theorem* (well known,[1,2] but written here for completeness) results immediately:

$$\bar{t} = \bar{\tau} + \mathrm{Arg}(f') \tag{I}$$

To go further, we take the second derivative:

$$f'' = \frac{d^2z}{d\zeta^2} = \left[\frac{d^2s}{d\sigma^2} + i\cdot\frac{ds}{d\sigma}\cdot\frac{d\bar{t}-d\bar{\tau}}{d\sigma}\right]\exp\left[i(\bar{t}-2\bar{\tau})\right] \tag{3}$$

and make use of Frénets' second formula, which reads,

$$\frac{1}{\bar{\rho}} = \frac{d\bar{\tau}}{d\sigma}, \qquad \frac{1}{\bar{r}} = \frac{d\bar{t}}{ds} \tag{4}$$

to get the following (see Appendix A):

Second theorem

$$\frac{1}{\bar{r}} = \frac{1}{|f'|}\times\left\{\frac{1}{\bar{\rho}} + \mathrm{Im}\left[\frac{f''}{f'}\exp(i\bar{\tau})\right]\right\} \tag{II}$$

Often, the basic contour is the unit circle, $\zeta=\exp(i\theta)$; then, $\bar{t}=\pi/2+\theta$, $\bar{\rho}=1$, and the above formulas simplify accordingly. (The author has been unable so far to find an explicit equivalent result in the available literature; the problem seems to have been put for the first time in 1932 by the great Romanian geometrist, G. Tzitzeica.[2,3])

III. Curvature Radius of a Streamline

Consider the flow pattern around a two-dimensional body (eventually obtained by conformal mapping from a circle, Figs. 2b and 2c). The complex potential F can be thought of as a conformal mapping of the flowfield ($\zeta=\xi+i\eta$) onto the complex plane $F=\Phi+i\Psi$, the body contour being mapped onto a cut along the $\Psi=0$ axis (Fig. 2a); the streamlines correspond to the horizontals $\Psi=$ constant, whereas the verticals $\Phi=$ constant represent the equipotential lines. We pose the following problem: is it possible to calculate the radius of curvature $\overline{\rho_s}$ of a streamline in the physical plane ζ? Formula (II) applies immediately, but one notices that the curvature of the line $\Psi=0$, in the complex plane F, is zero, so that we have to set $1/\bar{r}=0$ in Eq. (II), getting the following:

Received Feb. 7, 1991; revision received July 12, 1991; accepted for publication July 12, 1991.

*Senior Scientific Counselor, Aerodynamics; currently, Invited Professor, Université de Provence, SETT-MHEQ, Case 321, 13397 Marseille, France.

The author dedicates this work to the memory of his beloved Master, Elie Carafoli (1901-1983), whose high scientific and moral stature has been an inspiration for many of his pupils during an exceptionally dark period in the history of their land.

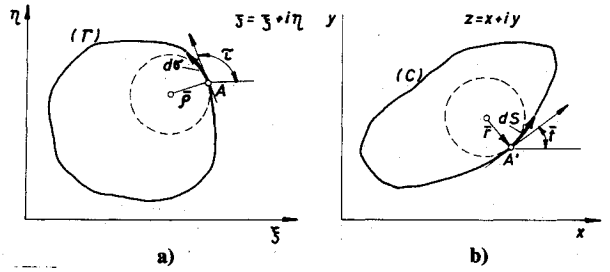

Fig. 1 Correspondence of two contours by conformal mapping.

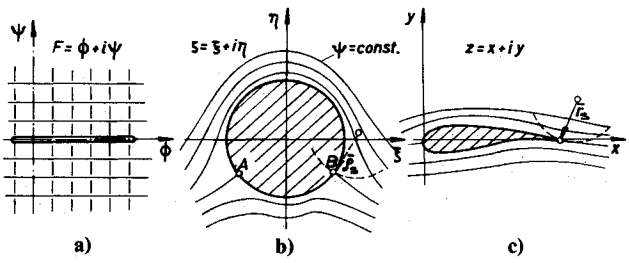

Fig. 2 Determination of the curvature radius of a streamline.

Third theorem

$$\frac{1}{\overline{\rho_s}} = -\mathrm{Im}\left[\frac{F''}{F'}\exp(i\bar{\tau})\right] \qquad \text{(III)}$$

For a body of arbitrary shape (e.g., an airfoil, Fig. 2c), the streamlines will be the images, in the complex plane $z = x + iy$, of those around the circle, by the same transform, $z = f(\zeta)$, that maps the airfoil contour. Then, to obtain the curvature radii of the streamlines in the transformed plane, one has to apply Eqs. (II) and (III) in succession, resulting in the following formula:

$$\frac{1}{\overline{r_s}} = \frac{1}{|f'|}\,\mathrm{Im}\left[\left(\frac{f''}{f'} - \frac{F''}{F'}\right)\exp(i\bar{\tau})\right] \qquad \text{(IIIa)}$$

IV. Conformal Mapping of Airfoils Having Different Trailing Edges

This problem has been extensively treated in the literature.[4-8] Here we shall insist only on some particular properties of the mapping function, imposed by the trailing-edge (TE) geometry. One can distinguish three basic configurations:

1) The contour is closed and cusped (Fig. 3a); i.e., the upper and lower surface tangents coincide at the TE (although the local radii of curvature may differ). This case is traditionally referred to as the Joukowsky type.

2) The TE is pointed, with a finite included angle δ (Fig. 3b); this is commonly named the Karman-Trefftz airfoil.

3) The TE is blunt, of thickness h (Fig. 3c); we shall call this class Carafoli-Whitcomb airfoils (see Refs. 9 and 10). In fact, if the boundary-layer thickness is added to the solid contour of any airfoil, the resulting equivalent airfoil can always be treated as being of this type (but its shape will change with the incidence).

Whatever the actual formulation employed, the conformal mapping requires four main steps; denoting z as the physical plane and ζ the final plane of the unit circle, one proceeds as follows:

1) Closing the contour (if needed): an elegant solution has been given by Garabedian,[1] who writes a mapping function whose derivative possesses a period in the intermediate transformed plane z_1. It is convenient to slightly modify Garabedian's function, so as to make the resulting, closed airfoil to feature a cusped TE. We shall not dwell upon these matters,

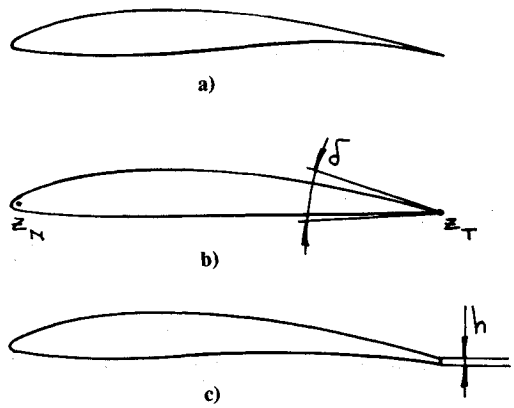

Fig. 3 Classification of airfoils by their trailing-edge shape: a) Joukowsky; b) Karman-Trefftz; c) Carafoli-Whitcomb.

but will point out that this mapping function is regular on the airfoil contour and in the whole domain outside.

2) Removing the angularity at the TE: a convenient general transform performing this task is the Karman-Trefftz function, which may be written as follows,

$$\frac{z_2 - z_{2T}}{z_2 - z_{2N}} = \left(\frac{z_1 - z_{1T}}{z_1 - z_{1N}}\right)^{1/k} \qquad (5)$$

where $k = 2 - \delta/\pi$. For a Joukowsky airfoil, $1/k = \frac{1}{2}$. Here, z_{1T} is the complex coordinate of the TE in the z_1 plane, z_{2T} is its image in the transformed plane z_2, and z_{1N} is a point, taken inside the airfoil contour, close to the nose (see Fig. 3b). The images z_{2T} and z_{2N} have to be conveniently taken to preserve the correct asymptotic behavior of the transform [i.e., $\lim (z_2/z_1) = 1$]. If the parameters of this transform are well chosen (see Ref. 8), the resulting contour is smooth (without any angular point) and very close to a circle.

3) Mapping the contour onto the unit circle $|\zeta'| = 1$: various methods are in use for this transform, one of the most powerful being that of Theodorsen[6-8]; this function is also regular along the contour.

4) Finally, it is convenient to set the image of the TE at $\zeta = 1$; this involves a rotation with an angle α_0, the zero-lift angle of attack of the airfoil: $\zeta = \zeta' \exp(i\alpha_0)$. In practice, it may be necessary to take several intermediate steps in the sequence of transforms, but all of their mapping functions are regular.

As the derivative of the overall mapping function, $f' = \mathrm{d}z/\mathrm{d}\zeta$, is obtained by taking the product of the derivatives of the successive transforms, it follows from the previous discussion that the behavior of f' near the TE is dominated by that of the derivative of Eq. (5), $\mathrm{d}z_1/\mathrm{d}z_2$ (since all of the other derivatives are regular there); we also note that this transform must always be present, whatever the airfoil type. It can be shown that, as z_1 is moved along the upper surface toward the TE, the modulus of this derivative tends to zero as $(s - s_0)$ raised to the power $(1 - \delta/\pi)/(2 - \delta/\pi) \leq \frac{1}{2}$ (s is the curvilinear abscissa along the contour); for a Joukowsky airfoil, one gets $|\mathrm{d}z_1/\mathrm{d}z_2| \to 0$ as $\mathrm{sqrt}(s - s_0)$. In the following, we shall suppose that the mapping function $z = f(\zeta)$ of the airfoil being considered is known, as well as its first and second derivatives, and we shall keep in mind the previous remarks about their behavior at the TE.

V. Flow Velocity at the Trailing Edge

Let α_∞ be the angle of attack of the undisturbed velocity U_∞, and put $\alpha = \alpha_\infty - \alpha_0$. Then, the complex potential, in the plane of the unit circle (and with the rear stagnation point set, as mentioned, at $\zeta = 1$), is written as

$$F(\zeta) = \exp(-i\alpha).\zeta + \exp(i\alpha)/\zeta + (i\Gamma/2\pi).\ln\zeta \qquad (6)$$

where the Kutta theorem gives

$$\Gamma = 4\pi \sin\alpha \tag{7}$$

The velocity in the ζ plane is

$$\frac{w_c(\zeta)}{U_\infty} = \mathrm{Conjg}\left(\frac{dF}{d\zeta}\right)$$

$$= \mathrm{Conjg}\left[\frac{\exp(-i\alpha)-\exp(i\alpha)}{\zeta^2} + \frac{(2i\sin\alpha)}{\zeta}\right] \tag{8}$$

To obtain the velocity $w(z)$ in the physical plane, one has to multiply w_c with the product of the derivatives of all of the successive mapping functions. This product can be written, keeping into account the previous discussion, as follows:

$$\frac{d\zeta}{dz} = \frac{d\zeta}{d\zeta'} \times \frac{d\zeta'}{dz_2} \times \ldots \times \frac{dz_1}{dz} = \frac{dz_2}{dz_1} \times g(\zeta) \tag{9}$$

Here we have set aside the derivative of the Karman-Trefftz transform, which is singular, and grouped together [and symbolically denoted by $g(\zeta)$] all of the other regular derivatives. Then, Eq. (8) becomes

$$\frac{w}{U_\infty} = \mathrm{Conjg}\left(\frac{dF/d\zeta}{dz_2/dz_1}\right) \times g(\zeta) \tag{10}$$

At the TE the ratio in Eq. (10) results in an indeterminacy, which can be lifted by l'Hospital's rule. Denoting

$$ZFACTOR = \mathrm{Conjg}\left\{\lim_{\zeta\to 1}[g(\zeta)]\right\} \tag{11}$$

one obtains, finally, the following:

Fourth theorem (i) In potential flow, the velocity at the trailing edge of an airfoil, having a cusped ($\delta = 0$) or a blunt shape there, is

$$w_{TE}/U_\infty = ZFACTOR \times \cos\alpha \tag{IV}$$

(ii) while, for a pointed airfoil ($\delta \neq 0$)

$$w_{TE} = 0 \tag{IVa}$$

Computations in actual cases give values of ZFACTOR of the order of unity (ZFACTOR = 1 exactly for the flat-plate airfoil); the velocity at the TE is almost always lower than that of the undisturbed flow.

VI. Formula for the Velocity Gradient

In the general case, let $F(z)$ be the complex potential of the flow around a two-dimensional body; the velocity along its contour may be written as,

$$\mathrm{Conjg}(w) = \frac{dF}{dz} = |w|\ \exp(-i\bar{t}) \tag{12}$$

By taking the second derivative, and making use of the formulas deduced previously, one obtains the following:

Fifth theorem

$$\frac{d|w|}{ds} = \mathrm{Re}\left[\frac{d^2F}{dz^2}\exp(2i\bar{t})\right] \tag{V}$$

Usually, the complex potential is written in the plane of the unit circle (ζ), and the second derivative in Eq. (V) has to be computed by the usual concatenation rule:

$$\frac{d^2F}{dz^2} = \left[\frac{d^2F}{d\zeta^2} - \frac{dF}{d\zeta}\cdot\frac{d^2z}{d\zeta^2}\Big/\frac{dz}{d\zeta}\right]\Big/\left(\frac{dz}{d\zeta}\right)^2 \tag{13}$$

It should be remarked that Eqs. (V) and (III) are pointwise formulas and, therefore, are (theoretically) free of numerical differentiation errors. Tests have actually shown that, especially near the leading edges of thin airfoils, radii of curvature, as well as velocity gradients, computed by finite differences may typically err by up to 30%, even if over 500 points are taken along the contour.

The results obtained so far lend themselves to manifold applications, such as the fine interpolation of the airfoil contour, to ensure a smooth distribution of the tangents and radii of curvature; also, to the preparation of input data for boundary-layer computations (which involve the velocity gradient), etc. Some more general consequences of these theorems will be taken up in the next section.

VII. Curvature of the Streamline at the Rear Stagnation Point

If, in Eq. (III) [or (IIIa)], we let the current point slide along the streamline emerging from the TE toward it, we obtain, in the limit, the value of the curvature of the flow at the tail. Several cases are of special interest.

A. Circular Body

Consider the flow around the unit circle (Fig. 2b): the value of the circulation Γ is related, by Eq. (7), to the polar angle α of the stagnation points A, B. Application of theorem III at point B produces an indeterminacy; after some tedious manipulations (see Appendix B), this can be lifted, obtaining the following:

Sixth theorem

$$1/\bar{\rho}_s = \tfrac{1}{3}\tan\alpha \qquad (\alpha \neq \pi/2) \tag{VI}$$

The case $\alpha = \pi/2$ requires a separate treatment, which may be carried out using the same technique as described in Appendix B. (The author is indebted to one of his reviewers for pointing out the singularity of this limit case.) Now the two stagnation points A, B coincide (Fig. 4) and one obtains the doubly singular limit

$$1/\bar{\rho}_s = \tfrac{1}{2} \qquad (\alpha = \pi/2) \tag{VIa}$$

Moreover, the two streamlines cease suddenly to emerge perpendicularly from the circle contour, to make a finite angle (60 deg) between them, and $\lim(\beta) = 30$ deg. A careful topological analysis, upon which we shall not dwell, confirms that this is, indeed, the correct configuration in this case.

These results are also readily checked by direct numerical experimentation: to this purpose, one takes several ζ points

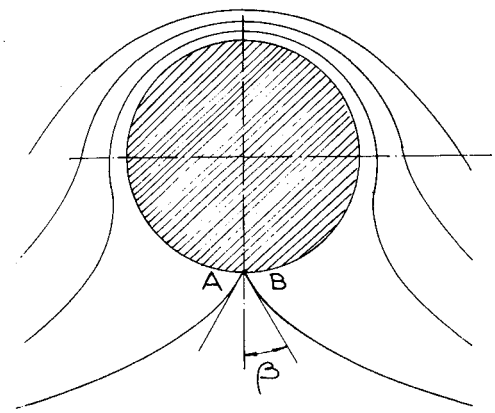

Fig. 4 Streamlines around a circle with stagnation-point polar angle set at $\pi/2$ rad.

along the streamline and one computes the complex potential and its derivatives; then, one can follow the value of the radius as it approaches its limit, given by Eq. (VI). The singular nature of the case $\alpha = \pi/2$ is vividly emphasized.

B. Flat-Plate Airfoil

For this classical case, the mapping function is simple:

$$z = f(\zeta) = \zeta + 1/\zeta, \quad f' = 1 - 1/\zeta^2, \quad f'' = 2/\zeta^3 \qquad (14)$$

The computation of $\overline{r_s}$ by Eq. (IIIa) can proceed in a similar way to that sketched in Appendix B; however, since at the TE $f' = 0$, one readily obtains the following:

Seventh theorem For a flat-plate airfoil,

$$1/\overline{r_s} = \infty \qquad (\alpha \neq 0) \qquad (VII)$$

This result is surprising and warrants further discussion; a detailed analysis shows that the streamline does, in fact, emerge tangentially from the trailing edge, but turns away at once. Actually, it takes the shape of a semicubic parabola ($y = x^{3/2}$), which is continuous, but has infinite curvature at the origin.

C. General Case of an Arbitrary Airfoil

In the general case (but with a TE of one of the types described in Sec. IV), we state the following:

Eighth theorem

$$\lim_{z \to z_{TE}} (1/\overline{r_s}) = \infty \qquad (\alpha \neq \alpha_*) \qquad (VIII)$$

The curvature at the trailing edge tends to infinity, to the possible exceptional case of a singular angle of attack.

To prove this statement, consider Eq. (IIIa): since, at the TE, $f'(z) = 0$ (see Sec. IV) in order for the curvature to remain finite, the term

$$T = \mathrm{Im}\left[(f''/f' - F''/F') \times \exp(i\bar{\tau})\right] \qquad (15)$$

should also tend to zero at the TE. But the ratio F''/F' depends only on α (F being the potential for the unit circle), whereas f''/f' is determined by the particular airfoil geometry (since it involves the derivatives of its mapping function). Therefore, T cannot be identically zero, for any α, to allow the curvature to remain finite. It also follows that a singular value α_* may exist that would render Eq. (IV) indeterminate. Using Eq. (VI) and keeping in mind that at the TE $\bar{\tau} \to 0$ (the tangent angle along the streamline in the circle plane), the requirement that $\lim(T) = 0$ results in the following equation:

$$\tfrac{1}{3}\tan\alpha = -\lim_{z \to z_{TE}} \left[\mathrm{Im}(f''/f')\right] \qquad (16)$$

whose solution $\alpha = \alpha_*$ represents the necessary (but not sufficient) condition for the streamline at the TE to have a finite curvature at this singular angle of attack.

D. Example: The Circular-Arc Airfoil

In the general case, the algebra is too complicated and, to find α_*, one must resort to numerical experimentation; but for certain simple shapes, the mapping function and its derivatives remain manageable. As an example, we have taken the circular-arc airfoil (Fig. 5); R is the arc radius, and a/c the bow. Following the same method of Appendix B, one finally finds that, indeed, $\overline{r_s} = 0$ for any α, except if,

$$\alpha = \alpha_* = -\tan^{-1}\left[(9/2)a/c\right] \qquad \text{when} \quad \overline{r_s} = R \qquad (17)$$

and the streamline emerges as a prolongation of the airfoil itself. Since α_* is negative, the airfoil has been drawn inverted in Fig. 5.

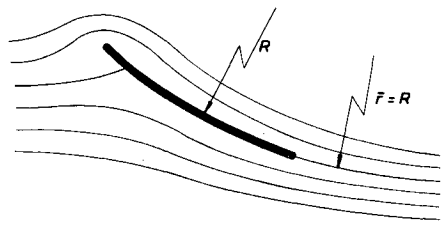

Fig. 5 Streamlines around a circular-arc airfoil at its singular angle of attack.

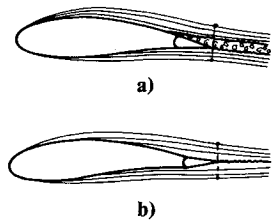

Fig. 6 Adjustment of the boundary-layer development to satisfy the requirement of finite streamline curvature: a) with the formation of a separation zone; b) with separation avoided by TE shape adaptation.

VIII. Discussion

The results accumulated so far allow us to discuss in some detail the real behavior of the flow near the TE, keeping into account the viscous effects. We shall start, as is customary, from the pressure distribution predicted by the inviscid analysis as an input to a boundary-layer program.

1) In the case of a pointed airfoil, as deduced in Sec. V, $w(\mathrm{TE}) = 0$; actual computations show that, near the edge, a region of strong adverse gradient is theoretically predicted. Moreover, the extent of this region is greater the higher the included angle δ. We state, therefore, that, computed from the inviscid pressure distribution, on a pointed airfoil, the boundary layer must always show separation.

2) For a cusped airfoil, we have seen that the trailing-edge velocity is nonzero; one would infer that, at the TE, separation is not necessarily present (unless, of course, the angle of attack is too high and detachment occurs anyway). However, theorem VIII says that the streamline curvature, at the TE, is infinite. On the other hand, theorem V [and Eq. (13)] shows us that, albeit in a way that cannot be explicitly formulated, the velocity gradient is directly dependent on the local curvature radius. It follows that, even for cusped airfoils, the boundary layer, as determined from the inviscid pressure distribution, must exhibit separation at least a short distance upstream of the trailing edge. In fact, ordinary boundary-layer computations involve a parabolization of the full Navier-Stokes equations; under these assumptions, any upstream influence of a singularity in the velocity distribution is lost, and the expected separation might not be properly recovered. Therefore, in the vicinity of the TE, such a formulation must be replaced with a more exact one (e.g., the triple deck).

3) In the case of blunt airfoils, the velocities on the upper and lower surfaces, at the TE, need not be zero, and, apparently, separation could be avoided (to the exception, obviously, of the dead-water zone behind the trailing-edge proper). However, the streamline curvature discontinuity is still present, and the above argument remains in force.

In reality, of course, the flow around the airfoil settles as the result of an interplay between the external field and the boundary-layer development, which modifies the pressure distribution; computer programs built on these lines are now common. It is convenient for our discussion to adopt the displacement-thickness concept and to consider a potential flow around the fattened blunt airfoil (Figs. 6). Now, as explained earlier, even for such a configuration, the curvature of the streamlines emerging from the upper and lower surfaces, at the TE, results

zero. This situation is, however, unacceptable on physical grounds; in a real flow, the curvature along the streamlines must be continuous. We infer that, in a certain way, there must be a mechanism whereby this is achieved. Although a formal proof seems difficult to establish, we are led, therefore, to state the following:

Ninth proposition In a real flow, at each angle of attack α, the interplay between the outer potential flow and the boundary-layer development will take place in such a manner as to produce an equivalent airfoil shape (including the displacement thickness), whose singular angle of attack α_* (which renders the streamline curvature finite), coincides with the actual α.

The resulting necessary thickening of the boundary layer at the rear, to satisfy this proposition, might not always involve a local separation, but this depends on the shape of the initial (solid) airfoil and, of course, on the incidence. The example given in Sec. VII.D. shows that to get this result the equivalent fluid airfoil should feature, at the rear, a negative camber; we have sketched two contrasting shapes and the consequent dead-water development in Figs. 6.

It follows that the familiar hooked shape of certain modern airfoils (including some supercritical designs) is almost invariably plagued with a small separated zone at the rear, even for low angles of attack; and, indeed, careful experimental pressure distributions recorded by the author in a large Ludwieg tube[11] on a number of typical airfoils have always revealed the presence of a small presure plateau over the last few percents of the chord. This may explain, perhaps, the failure of some airfoil designs to fulfill their expected performance.

This led us to think that, by properly shaping the airfoil TE (with a small negative camber there), one might get a beneficial effect, perhaps of a few percent, on the shape drag; also, the lift-curve slope might be improved. Since, however, at higher angles of attack, a hooked shape is requested for other reasons, a small moving tab, as indicated in Fig. 6b, could do the job of adjusting the TE camber and reduce cruise drag. The author's attention has been drawn[12] to the practice of a small negative flap setting on sailplanes in high-speed cruise. In addition to other effects, the phenomena discussed herein might contribute to the experienced drag reduction. We believe that the possible improvement offered by such a solution might be comparable with that expected from some more exotic (and costly) boundary-layer manipulations.

Of course, at higher angles of attack, the boundary-layer will separate anyway; we have reasons to believe that the proposed configuration might prove beneficial in this situation also.

Appendix A: Derivation of Theorem II

From Eq. (2), one gets

$$\frac{ds}{d\sigma} = |f'| \tag{A1}$$

One may also write

$$\frac{d\bar{t}}{d\sigma} = \frac{d\bar{t}}{ds}\cdot\frac{ds}{d\sigma} = \frac{1}{\bar{r}}\cdot|f'| \tag{A2}$$

Equations (4) can then be rearranged to read

$$f'' = \left\{\frac{d^2s}{d\sigma^2} + i|f'|\times\left[\frac{1}{\bar{r}}\cdot|f'| - \frac{1}{\bar{\rho}}\right]\right\}\times\frac{f'}{|f'|}\exp(-i\bar{\tau}) \tag{A3}$$

or

$$A + iB = \frac{f''}{f'}\exp(i\bar{\tau}) - \frac{d^2s/d\sigma^2}{|f'|} = i\left[\frac{1}{\bar{r}}|f'| - \frac{1}{\bar{\rho}}\right] \tag{A4}$$

Since the second term in the left-hand side is real, one obtains

$$B = \mathrm{Im}\left[\frac{f''}{f'}\exp(i\bar{\tau})\right] = \frac{1}{\bar{r}}\cdot|f'| - \frac{1}{\bar{\rho}} \tag{A5}$$

from where theorem II follows immediately.

Appendix B: Derivation of Theorem VI

The complex potential [Eq. (6)] is slightly rearranged to read

$$F(\zeta) = \zeta + 1/\zeta + 2i\,\sin\alpha\cdot\ell n\zeta = \Phi + i\Psi \tag{B1}$$

The stagnation points A, B (Fig. 2b) are set at polar angles $\pi+\alpha$ and $-\alpha$, respectively. One takes a point P, along the streamline emerging from B, defined as

$$\zeta_P = \rho\exp\left[i(\varphi-\alpha)\right] \qquad (\rho\geq 1) \tag{B2}$$

At B, $\rho=1$, $\varphi=0$. The condition that P should lie along the streamline is obtained by replacing Eq. (B2) in Eq. (B1) and equalling to zero the imaginary part of the complex potential; this results in the following relation between φ and ρ, valid along the streamline:

$$\sin(\varphi-\alpha) = -\sin\alpha\,\frac{2\rho\cdot\ell n\rho}{\rho^2-1} \tag{B3}$$

On the other hand, one has

$$d\zeta = d\sigma\exp(i\bar{\tau}) = (d\rho + i\rho\,d\varphi)\exp\left[i(\varphi-\alpha)\right] \tag{B4}$$

from which one deduces

$$\bar{\tau} = \varphi - \alpha + \beta \tag{B5}$$

where, using also Eq. (B3),

$$\tan\beta = \rho\frac{d\varphi}{d\rho} = \frac{2\rho\,\sin\alpha}{\cos(\varphi-\alpha)}\cdot\frac{(\rho^2+1)\cdot\ell n\rho - (\rho^2-1)}{(\rho^2-1)^2} \tag{B6}$$

From Eq. (B1):

$$\frac{F''}{F'} = \frac{2}{\zeta}\cdot\frac{1-i\zeta\sin\alpha}{\zeta^2-1+2i\zeta\sin\alpha} \tag{B7}$$

Replacing, in Eq. (B7), ζ by its expression (B2), keeping account of Eqs. (B3), (B5), and (B6), and carrying everything into Eq. (IV), one obtains a relation of the form $1/\overline{\rho_s} = \mathrm{Funct}(\rho,\alpha)$. At the stagnation point, this equation becomes indeterminate; use of l'Hospital's rule is extremely awkward and, to lift the indeterminacy, it is more convenient to set $\rho = 1+\epsilon$ and to develop in series all of the expressions involved. Care must be taken to retain a sufficient number of terms in the developments; as an example, we give the equivalent of Eq. (B3):

$$\sin(\varphi-\alpha) = -\sin\alpha\cdot(1 - 1/6\epsilon^2 + 1/6\epsilon^3 - 2/15\epsilon^4 + \cdots) \tag{B8}$$

After some tedious algebra, one finally can set $\epsilon\to 0$ to reach Eq. (VI).

References

[1]Bauer, F., Garabedian, P., and Korn, D., *Supercritical Wing Sections,* Lecture Notes in Economics and Mathematical Systems, Vol. 66, Springer-Verlag, New York, 1972.

[2]Jacob, C., *Introduction Mathématique à la Mécanique des Fluides,* Gauthier-Villard, Paris, 1951.

[3]Tzitzeica, G., "Sur la Représentation Conforme," *C. R. Acad. Sc. de Paris,* Vol. 195, 1932, pp. 476, 478.

[4]Carafoli, E., *Aérodynamique des Ailes d'Avion,* Chiron Ed., Paris, 1928.

[5]Carafoli, E., *Tragflügeltheorie,* VEB Verlag Technik, Berlin, 1954 (translation of the Romainian original *Aerodinamica,* Editura Technica, Bucharest, 1951).

[6]Müller, W., "Construktion von Tragfachenprofilen," *Zeitschrift für angewandte Mathematik and Mechanik,* Vol. 218, 1924.

[7]Theodorsen, T., and Garrick, I. E., "General Potential Theory of Arbitrary Wing Sections," NACA TR 452, 1933.

[8]Ives, D. C., "A Modern Look at Conformal Mapping, Including Multiply-Connected Regions," *AIAA Journal,* Vol. 14, No. 8, 1975, pp. 1006–1011.

[9]Carafoli, E., "Sur les Profils Aérodynamiques de Forme Générale," *C. R. Acad. Sc. de Paris,* Vol. 185, 1927, p. 1014.

[10]Milne-Thompson, L. M., *Theoretical Aerodynamics,* Macmillan, London, 1948.

[11]Dumitrescu, L. Z., "A Large-Scale Aerodynamic Test Facility, Combining the Shock and Ludwieg-Tube Concepts," *Shock Tubes and Waves, Proceedings of the XII International Symposium on Shock Tubes and Waves,* edited by A. Lifshitz and J. Rom, Magues, Jerusalem, 1980, pp. 137–146.

[12]Dumitrescu, M. P., private communication.